International Journal of Disaster Risk Reduction 31 (2018) 832–843

Contents lists available at ScienceDirect

International Journal of Disaster Risk Reduction

journal homepage: www.elsevier.com/locate/ijdrr

# Framework for improving the resilience and recovery of transportation networks under geohazard risks

Nazli Yonca Aydin[a,*], H. Sebnem Duzgun[b], Hans Rudolf Heinimann[a], Friedemann Wenzel[c], Kaushal Raj Gnyawali[d]

[a] ETH Zurich, Future Resilient Systems, Singapore-ETH Centre, 1 CREATE Way CREATE Tower, Singapore 138602, Singapore
[b] Colorado School of Mines, Dept. of Mining Eng., 1500 Illinois Str., 80401 Golden, CO, USA
[c] Karlsruhe Institute of Technology, Geophysical Institute, Hertzstr. 16, 76187, Karlsruhe, Germany
[d] Shanghai Jiao Tong University, Department of Civil Engineering, School of Naval Architecture, Ocean and Civil Engineering, Shanghai 200240, China

ARTICLE INFO

*Keywords:*
Disaster resilience
Debris clearance
Earthquake-triggered landslides
Graph theory
Resilience strategies
Transportation network

ABSTRACT

Rural transportation networks are highly susceptible to geohazards such as earthquakes and landslides. Indirect losses can be severe because the breakdown of a transportation network aggravates rescue, supply, and other recovery activities. The operations and logistics of rural networks that are under seismic risks must be managed using the limited resources specifically in developing countries. We propose a methodology to evaluate road recovery strategies for restoring connectivity after blockages due to earthquakes and earthquake-triggered landslides. This paper gives insight into the recovery process, which can be used by decision-makers for enhancing resilience and supplying immediate relief to rural areas. The proposed framework has four steps: 1) identification of strategies for increasing recovery performance, 2) determination of graph-based metrics to represent network connectivity, 3) applying topology-based and Monte Carlo simulations to each strategy, and 4) analysis of recovery times to compare these resilience-enhancement strategies. The methodology was tested using a case study from Sindhupalchok District, Nepal, a region that was severely affected by the Gorkha earthquake in 2015. The closed road segments and recovery times were determined through field surveys with locals and governmental authorities, and by investigating the intensity of earthquake-triggered landslides. Our results showed that the proposed approach provides information about the recovery behavior of road networks and simplifies the evaluation process. It is robust enough to extend and assess decision-makers' preferences for improving resilience.

## 1. Introduction

Although its definition can vary across disciplines, resilience is most commonly considered an element of risk assessment. The resilience of critical infrastructure refers to recovery or the self-healing capacity to become fully or partially operational after a disruption due to natural or human-made impacts that arise from physical or cyber threats. The National Academy of Sciences [31] describes disaster resilience as a systems' capability "to prepare and plan for, absorb, recover from, or more successfully adapt to actual or potential adverse events." The Sendai Framework for Disaster Risk Reduction 2015–2030 [40], composed by the United Nations Office for Disaster Risk Reduction, explicitly addresses the need for methodologies and tools for reducing risks by strengthening the resilience of an infrastructure.

Transportation networks are a backbone of critical infrastructures because they provide accessibility to the other systems and rescue operations immediately after a disaster strikes and during restoration processes. Therefore, enhancing resilience and understanding the complexity of recovery behavior are crucial for transportation networks, which can be analyzed and evaluated through decision alternatives for an agile recovery.

In some cases, the recovery process for transportation networks after natural disasters is investigated as a problem of debris-clearing, which is solved by optimization algorithms [39,8]. Even though the formulation of such optimization problems takes uncertainties into account in allocating resources, and could facilitate some basic understanding of infrastructure resilience, it does not provide real solutions in some situations. For example, during short-term recovery,

* Corresponding author.
*E-mail addresses:* nazli.aydin@frs.ethz.ch (N.Y. Aydin), duzgun@mines.edu (H.S. Duzgun), hans.heinimann@env.ethz.ch (H.R. Heinimann), friedemann.wenzel@kit.edu (F. Wenzel), gnyawalikr@sjtu.edu.cn (K.R. Gnyawali).

https://doi.org/10.1016/j.ijdrr.2018.07.022
Received 22 May 2018; Received in revised form 25 July 2018; Accepted 26 July 2018
Available online 30 July 2018

infrastructure systems may not fully recover whereas the long-term recovery capacity becomes better than the original capacity after the disruption via network enhancement. In such cases, the formulation of the optimization problem should be different than reaching to the full operational capacity.

For transportation infrastructure in particular, baseline functionality cannot be achieved in the midst of massive destruction due to geohazards such as landslides and earthquakes. However, even greater results might be possible in the long run if some parts of the transportation network are rebuilt to handle larger capacity or if the network topology is enhanced by the rearrangement/addition of nodes. Although fully operational capacity might not be possible, an agile recovery to some degree of functionality would be acceptable and would indicate resilience for infrastructure operators in effectively supplying relief efforts. When such infrastructures have better operational capacity due to replacement and/or improvement after natural disasters, the resource allocation problem should be formulated to incorporate a spatiotemporal scale and associated parameters. Therefore, understanding and measuring the complex nature of infrastructure resilience within an operational context necessitates a systematic evaluation of various decision alternatives.

In addition to optimization approaches, network theory has been used to assess infrastructure resilience. For example, Schintler et al. [37] have proposed a method for transportation networks that utilizes graph-based metrics (e.g., average path length, betweenness centrality). Another probabilistic resilience evaluation focuses on multiple infrastructure systems and their dependencies [5]. Aydin et al. [2] have previously proposed a resilience evaluation method for transportation network topology that integrates graph-based metrics into stress-testing methodologies. Ayyub [3] has provided a detailed overview of the definitions of resilience used within the context of ecology, social sciences, natural hazards etc., as well as the metrics that were available. However, evaluation methods associated with network theory are limited to structural performance. To our knowledge, no reports have been made on the time-variable recovery performance of networks for evaluating different strategies.

As an alternative, probabilistic models are used to investigate infrastructure functionality losses under single or multiple natural or human-made hazards. For example, Shangyao et al. [38] have applied scenario analysis to restore road segments, prioritizing based upon restoration demands. In a study of earthquakes, Ertugay et al. [17] devised a probabilistic accessibility method for identifying road closures in an earthquake case study. Lam and Adey [28] have assessed restoration and functional capacity losses using a probabilistic approach for the road network in the city of Basel. Their research was aimed at examining the indirect consequences that stakeholders should consider for the purposes of risk reduction and disaster management. Some of these methods are not directly related to the resilience of road networks (e.g. [17]). Furthermore, these evaluation approaches involve a high level of expert knowledge, cost or increased computation time which is not readily available in developing countries (e.g. [28,38]).

Certain optimization methods for recovering road segments are based on objectives such as minimum operation costs [43]. More complex algorithms focus on minimizing restoration time and distribution of relief supplies. Due to the complexity of objectives, the problem is handled by sub-dividing it into smaller sections. The main issue with such complexity is that applying those solutions requires expertise and computational efficiency. In many developing countries, after natural disasters such as earthquakes, floods, and landslides, resources and/or time are inadequate for implementing those complex applications. Furthermore, the decision-makers must quickly understand the problem and respond accordingly with a solution in a fast manner.

In order to tackle the above-mentioned challenges related to the transportation infrastructure resilience, this study proposes a framework that will assist in understanding the road recovery behavior in rural areas under natural disasters. The framework aims to reduce complexities while considering the uncertainties in recovery processes. The performance of alternative road recovery strategies, as identified through a literature review and stakeholder interviews, was investigated via topology-based simulations that used a graph-based connectivity metric called Giant Connected Component (GCC). Each strategy was investigated in terms of its ability to decrease the mean recovery time, the efficiency of the recovery process, and magnitude of uncertainty, which was evaluated at the entire network scale. Monte Carlo Analysis was applied to quantify the uncertainty during the recovery process. To demonstrate the successful implementation of our proposed approach, we established a case study for the Sindhupalchok District in Nepal. Due to an earthquake and major aftershock in 2015 (magnitude of 7.8 and 7.3, respectively), the rural transportation network in that district was severely damaged, thereby having an adverse impact on the accessibility of relief efforts.

The proposed work is novel in terms of allowing decision-makers to assess the performance of road recovery strategies; therefore, the highest level of resilience enhancement can be easily identified. It combines an intuitive decision-making process for characterizing resilience enhancement strategies with analytic modeling in order to improve the understanding of a recovery behavior and operational resilience. In addition, this approach reduces the computation time and enables easy understanding for decision-makers. It is also flexible in taking decision-makers' preferences into account. In case decision makers and stakeholders wish to include another strategy, the corresponding recovery functions can be produced promptly after determining the sequence of road recovery. Its successful implementation in a real case study illustrates its capability in capturing the needs of decision-makers, which is also a technical merit. Moreover, the proposed approach characterizes theoretical resilience functions for a given infrastructure, which then enables decision-makers to plan for effective strategies for resilience enhancement.

## 2. The framework

In addition to data collection and processing, our proposed framework has four main steps (Fig. 1): 1) identification of realistic road recovery strategies; 2) determination of the measure of performance (MOP) for representing road network connectivity, using a graph-based metric; 3) simulations for evaluating topology for a given transportation network and strategies, and Monte Carlo simulations analyzing uncertainty in recovery times; and 4) evaluation of MOPs to compare strategies in terms of resilience, which are carried out based on the simulation results expressed in terms of recovery time.

### 2.1. Identification of strategies

A set of road recovery strategies that can improve the overall resilience of rural transportation networks under disruptions was proposed.

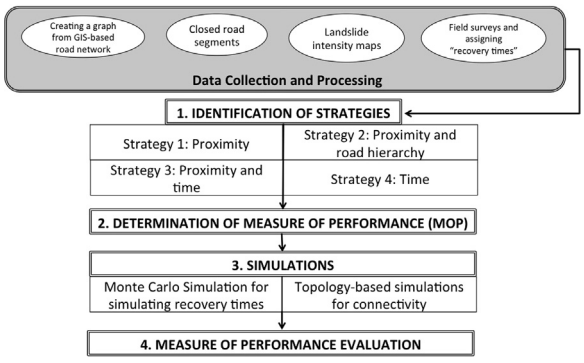


**Fig. 1.** Proposed framework.

The main disruption examined here was road closures due to earthquake-triggered landslides. Such strategies depend upon the availability of resources and the priorities that are set for restoring functionality within a rural area. Various factors must be considered when determining the road recovery sequence: proximity to resources, road hierarchy, and time required for clearing the road.

In this study, the clearing time for each closed road segment was based on the amount of debris blocking that road segment, the severity of accidents (if any), and work schedules of clearance teams for dispatching the closed road segments. Road clearance becomes especially an utmost challenge in mountainous areas, where accessibility of relief efforts is required to be maintained for fast and efficient recovery in case of a large number of road blockages due to landslide debris or accidents. We evaluated four strategies that were selected based on relevant literature and focus group meetings that were conducted by road authorities.

Strategy 1 involved a road recovery strategy using a single variable "proximity to the main resource center" and assumed that humanitarian logistics and emergency management services could access a rural area from the nearest metropolitan region. Here, our main purpose was to reach the destination by the shortest route. A similar strategy has been tested within the optimization context by Maya Duque and Sörensen [30], who aimed to maximize accessibility to primary urban centers after natural or man-made disasters. Whereas that earlier study focused on the search algorithm, our main objective was to restore the overall network connectivity rapidly.

Strategy 2 took road recovery into account based on two variables "proximity and road hierarchy". During the process of designing a transportation network, segments are generally categorized as primary, secondary, or minor roads. The underlying assumption is that restoring the most important, i.e., primary, road segments will provide faster recovery. Therefore, segments that are blocked by debris from earthquake-triggered landslides are restored based on 1) the hierarchical level of that particular segment and, 2) proximity to the main resource center. For example, primary segments closest to a resource center would be the first to receive attention, followed by secondary and then minor road segments, based on their proximity to a resource center.

Strategy 3 considered road recovery according to both proximity and time to recover. The time required to restore each closed segment was determined by the amount of debris on the road, by surveys with authorities. These surveys applied to identify their response time and operation capacity including the work schedules of clearance teams etc. Although the recovery time for each edge was used to configure cumulative recovery functions for all strategies, it was specifically geared toward sequencing roads for recovery in Strategy 3. Here, the focus is to clear road segments in an order that would take the least amount of time (e.g., the least amount of debris) and that are close to a resource center. Chang [10] has explored a similar strategy for restoring accessibility to railroad service after the 1995 Kobe earthquake in Japan. Here, we assessed the feasibility of this strategy based on recovery time needed to provide resilient rural transportation networks.

In Strategies 1, 2, and 3, intervention sequences for road clearance were determined based on pre-defined priorities, i.e., proximity, road hierarchy/proximity, or time/proximity. In contrast, Strategy 4 focused on dynamically simulating a sequence based on the time variable. First, the time required to open a closed road segment was identified by probability density functions (PDFs). Afterward, those segments were sorted in ascending order based on the identified time variable to determine the most suitable restoration sequence. Unlike Strategy 3, we completely omitted the proximity prerequisite and looked at only the time variable. We hypothesized that this approach would be helpful for decision-makers in terms of understanding the changes in recovery behavior under uncertainty. Fig. 2 shows how these strategies would work on a sample network.

Let $G(V,E)$ be an uc $n$ number of vertices and $m$ number of edges. The distance between any two vertices, $v_k$ and $v_l$, is called $D_{k,l}$ and is

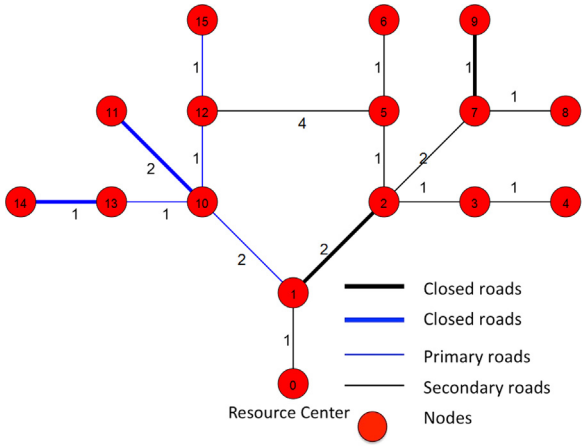


**Fig. 2.** The sample network has 16 nodes and 16 edges. The resource center is marked as 0 in the figure, $v_0$. Closed road segments are $e_{1,2}$, $e_{7,9}$, $e_{10,11}$, $e_{13,14}$; minimum time needed to open closed segments are 7, 1, 1, and 24 h, respectively. Edge lengths are dimensionless and given in the figure.

calculated by Dijkstra's algorithm. An edge, $e$, is named based on the adjacent nodes, such that $e_{i,j}$ is an edge which connects $v_i$ and $v_j$. Vertex $v_s$ is the resource node. Because it is more straightforward to find the shortest path from one vertex to another, we defined the shortest distance from resource center $v_s$ to blocked edge $e_{i,j}$ as $Min(D_{s,i}, D_{s,j})$, where $D_{s,i}$ is the shortest path from $v_s$ to $v_i$ and $D_{s,j}$ is the shortest path from $v_s$ to $v_j$. For the example in Fig. 2, the shortest paths from resource center ($v_0$) to the closed road segments $e_{1,2}$, $e_{7,9}$, $e_{10,11}$, $e_{13,14}$ were 1, 5, 3, and 4 units, respectively. Those paths passed through vertices [$v_0$, $v_1$], [$v_0$, $v_1$, $v_2$, $v_7$], [$v_0$, $v_1$, $v_{10}$], and [$v_0$, $v_1$, $v_{10}$, $v_{13}$], respectively.

Based on those above parameters, the road-opening sequence for Strategy 1 would be [$e_{1,2}$, $e_{10,11}$, $e_{13,14}$,$e_{7,9}$]; for Strategy 2, [$e_{10,11}$, $e_{13,14}$,$e_{1,2}$, $e_{7,9}$]; and for Strategy 3, [$e_{10,11}$, $e_{7,9}$, $e_{1,2}$, $e_{13,14}$]. While determining the sequences for strategies 1, 2, and 3 is relatively a straightforward process, for Strategy 4, it relies on simulating recovery times for each closed road segment using a PDF. The time and therefore the sequences were both changed in each simulation to quantify uncertainty. A sequence was determined by sorting the segments based on the time it would take to recover in ascending order (e.g. 1, 1, 7, 24 and so on).

Whilst strategies 1 and 4 required sequencing based on a single variable (i.e., either time or proximity), strategies 2 and 3 required consecutive sorting. For example, Strategy 2 was based on two variables; proximity and road hierarchy. While creating the road recovery sequence for this strategy, first priority was given to "road hierarchy", the second priority was given to "proximity" such that the closed road segments were first sorted based on their hierarchical level (i.e., highways, secondary road segments, third degree road segments), then in each hierarchical level (e.g., highways) road segments were sorted with respect to their proximity to the main resource center.

On the other hand, some strategies such as Strategy 3 implicitly considered recovering the lower hierarchical road segments before, if it blocked the access to the higher hierarchical road segments, because the proximity to a resource center and recovery time were considered in defining the sequence of road cleaning. For example, in Strategy 3 (i.e., road recovery using proximity and time to recover), the lower hierarchical road segment might be cleared before the higher priority road, if the time it takes to recover the corresponding road segment was less than higher hierarchical road segment and if it was closer to the resource, while in Strategy 2 (i.e., proximity and road hierarchy), the higher hierarchical road segments were always recovered before lower hierarchical road segments.

### 2.2. Determining measures of performance

Our current research is based on our premise that a common metric is needed to enable objective comparisons and express the performance of a network under each recovery strategy. Historically, graph-based metrics have been used to assess the topological properties of networks. Each metric can be meaningful for a specific purpose or type of network (e.g., social or physical). For example, centrality measures are taken to evaluate criticalities in networks. Degree centrality, the number of links to which a node is connected, is informative in social networks because it represents the number of people that one individual might know or share a link. However, a transportation network has spatial referencing as well as design rules and regulations, all of which restrict the number of possible connections for a node [20].

While centrality metrics can provide insight into the criticality levels of individual nodes, our study focuses on restoring connectivity at the entire network level. In this way, we can compare recovery times after implementing individual strategies. Connectivity metrics in complex network applications, such as spanning trees, clustering coefficients, or algebraic connectivity, are mostly used to characterize networks by counting triangles, and loops. Other metrics, e.g., alpha, beta, and gamma indices; diameter; or average path lengths; do not reflect the property of node-to-node connectivity in a network [16,23,29,34].

The Giant Connected Component (GCC) describes the size of the largest connected component within a network. It is one of the most common graph-based metrics for evaluating network resilience and/or robustness, and it represents the connectivity level of an entire network [33]. In the field of disaster management, network robustness has been defined by Bruneau et al. [6] as the operational range or disruption threshold that a particular system can tolerate. Furthermore, GCC is generally used to test robustness by removing nodes or links and examining the size of the largest surviving connected module in a network. This process of node removal can be either random, as described by Albert et al. [1], or a targeted attack. Callaway et al. [7] have used GCC to describe network robustness and percolation thresholds on random graphs. This metric is also applied to railway, air, and cargo transportation; communications; and multiplex networks to assess the robustness and/or resilience of networks and flow robustness [42,45,46,9].

For example, Aydin et al. [2] used the GCC along with betweenness centrality and network efficiency to evaluate the topological resilience of urban road networks under seismic hazards in the Kathmandu metropolitan region, Nepal. Even though it can serve as a common measure to represent the threshold of network percolation subject to random and/or malicious attacks, in this study, we used the GCC as a metric to estimate the connectivity performance of a network. Our goal was to understand whether one strategy is more effective than another in terms of recovery speed. Because it is essential that authorities preserve network connectivity to support rescue, supply, and reconstruction activities after geohazards, the GCC metric is valuable in evaluating strategies for resilience enhancement.

### 2.3. Simulations

The third step in this proposed framework was to apply topology-based network simulations for predicting network connectivity recovery for each strategy. Monte Carlo simulations were also used for determining the uncertainty in the recovery times associated with each strategy.

#### 2.3.1. Topology-based simulations

Topology-based simulations were modeled according to the requirements of each strategy and were evaluated using the igraph network analysis package with Python programming tools [24]. In this study, first, a rural transportation network was represented as a graph $G(N, L)$ with $N$ set of node and $L$ set of edges as an undirected and weighted network. Then, a disrupted rural road network was represented as a graph by removing the entire closed/disrupted road segments (i.e., edges) from the baseline road network. Later, these road segments were added back into network one by one and connectivity of networks (i.e., GCC) was calculated.

This procedure included adding a road segment, evaluating the GCC of the network, and normalizing it by the baseline GCC value. This step was repeated until all closed segments were restored. The sequence by which those segments were added was determined per strategy requirements (i.e., proximity, time/proximity, hierarchy/proximity, time). The GCC was normalized as follows:

$$Q_{network,t} = \frac{N_{GCC,t}}{N_{GCC,baseline}} \tag{1}$$

where $Q_{network,t}$ is the normalized GCC, $N_{GCC,baseline}$ is the initial size of the GCC for networks, and $N_{GCC,t}$ is the GCC size at time $t$.

#### 2.3.2. Monte Carlo simulation

Monte Carlo analysis is the most common method [25,26,35] for quantifying uncertainty because it allows using probabilistic models. It is based on examining a probability distribution to test a hypothesis by randomly selecting variables through repeated sampling. In order to have a higher accuracy, random sampling should be repeated a large number of times. Monte Carlo simulations are widely used for disaster management and risk evaluation. Yang et al. [44] have applied this technique to generate hazard events when investigating the criticalities in transportation networks under tropical hazards. Nelson and Grubesic [32] have used the Monte Carlo method to simulate mean estimates of oil spills on a shoreline while Ertugay and Duzgun [18] have applied this approach for modeling accessibility.

We conducted Monte Carlo simulations to represent the uncertainty in recovery times for each road segment. Although upper and lower bounds for each blocked segment were determined through surveys with authorities and field data that indicated the amount of debris on a road, there was uncertainty about how long it would take to clear and open that segment. Ultimately, cumulative recovery times for each strategy were calculated using the outcomes of these simulations.

The truncated, uniform and triangular PDFs were used for sampling values for time variable on a single strategy to determine a single method that will be applied to all strategies.

##### 2.3.2.1. PDF for truncated normal distribution.

$$f(x) = \begin{cases} 0 & \text{if } x \le a \\ \frac{\phi(\bar{\mu}, \bar{\sigma^2}; x)}{\phi(\bar{\mu}, \bar{\sigma^2}; b) - \phi(\bar{\mu}, \bar{\sigma^2}; a)} & \text{if } a < x < b \\ 0 & \text{if } b \le x \end{cases} \tag{2}$$

where, $\mu$ and $\sigma$ are the mean and variance of the "parent" general normal PDF, $a$ and $b$ are the upper and lower bounds for the truncation interval.

##### 2.3.2.2. PDF for uniform distribution.

$$g(x) = \begin{cases} \frac{1}{b-a} & \text{if } a \le x \le b \\ 0 & \text{otherwise} \end{cases} \tag{3}$$

where, $a$ and $b$ are the upper and lower bounds for the uniform interval.

##### 2.3.2.3. PDF for triangular distribution.

$$z(x) = \begin{cases} \frac{2(x-a)}{(b-a)(m-a)} & \text{if } a \le x \le m \\ \frac{2\ (b-x)}{(b-a)(b-m)} & \text{if } m \le x \le b \\ 0 & \text{otherwise} \end{cases} \tag{4}$$

where, $a$ and $b$ are the upper and lower bounds for the triangular

interval, and *m* is the mode scalar. The Monte Carlo Simulations were applied for Strategy 1 using these three different PDFs to eliminate the dependency of random draws on the probability distribution. To reduce the computation time, we chose only one PDF for the remaining strategies. The following procedure was adopted:

i. Determine the road recovery sequence based on proximity
ii. Add an edge based on that sequence
iii. Draw a random sample to represent recovery times for the closed road segments with a PDF
iv. Evaluate GCC
v. Evaluate cumulative recovery time
vi. Repeat 10,000 times

A slightly different procedure was used for Strategy 4:

i. Draw a random sample to represent recovery times for the closed road segments with a PDF
ii. Sort edges based on recovery times in ascending order to determine the road sequence
iii. Add road segments according to the order determined by sorting
iv. Evaluate GCC
v. Evaluate cumulative recovery time
vi. Repeat 10,000 times

### 2.4. Evaluation of MOP

Each strategy was evaluated based on its ability to restore overall connectivity (i.e., GCC) at the network level. The speed of recovery, or so-called "rapidity", has been the focus of evaluations for system resilience in the literature, as described by Ganin et al. [19]. This concept, first proposed by Bruneau et al. [6], has since then been modified to investigate specifically the "rapidity" dimension of resilience as it refers to the speed of recovery [14,21,4].

In our research, minimum and maximum restoration times for the closed/disrupted road segments were determined by three major factors: 1) the magnitude of earthquake-triggered landslides, 2) field surveys and interviews with the locals, and 3) the operational capacity of authorities and experience of locals and government employees. While those surveys included questions about average response times by road authorities, the magnitude of an earthquake-triggered landslide was used to estimate the amount of time needed to remove the debris from a disrupted road segment. This allowed us to evaluate the cumulative recovery times for strategies and enabled comparisons among them.

In this study, the performance of each strategy was evaluated by the following criteria: 1) mean final recovery time, 2) efficiency of the recovery process, and 3) magnitude of uncertainty. Fig. 3 exemplifies how recovery performance for a single strategy was measured according to those criteria.

The first criterion was fulfilled by establishing the mean final recovery time for each strategy. The range in times was calculated via Monte Carlo simulations and the output was represented with histograms. The mean final recovery time would specifically be an important measurement if only all road segments were not recovered and decision makers' and stakeholders needed to choose a set of road segments to recover.

The efficiency of a recovery process was measured by investigating the cumulative distribution functions (CDF) at each quartile of the recovery process. Here, we divided that process into 4 sections and considered 25% of all closed segments to be recovered within each section, then mean, maximum, and minimum recovery times for each section were recorded. If a strategy were more efficient than the others, the mean recovery time (i.e., $t_{mean}$ which is shown for example Strategy A in Fig. 3) at 25%, 50% and 75% of the recovery would be less than the other strategies (i.e., $t_{strategy\ A,\ mean} < t_{strategy\ B,\ mean}$).

In order to compare the magnitude of uncertainty, minimum and maximum recovery times (i.e., $t_{min}$ and $t_{max}$ which are shown for example Strategy A in Fig. 3) were compared at each quartile. This criterion is important to convey to decision makers who should take into account the uncertainty before implementing any strategy.

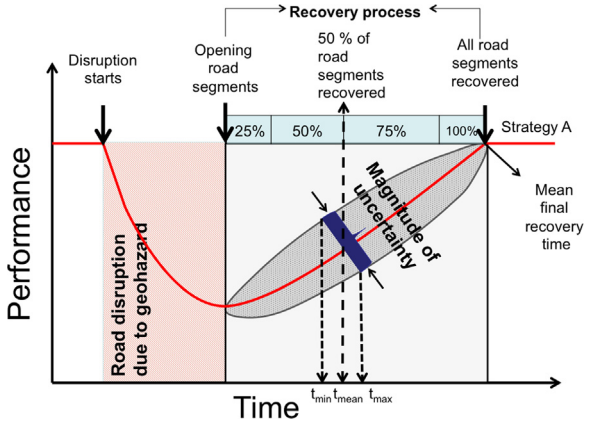


**Fig. 3.** Recovery performance evaluation. $t_{min}$, $t_{max}$, and $t_{mean}$ changed in each quartile based on a specified road clearance sequence, and serve only as an example for Strategy A, i.e., at 50% recovery.

## 3. Implementation within the Sindhupalchok District of Nepal

We applied the proposed framework to a rural road network located in Sindhupalchok District, Nepal. The 2015 Gorkha earthquake in the central part of that country caused extensive damage and hundreds of fatalities, and also triggered a large number of landslides, specifically in rural areas, where it had ramifications on their transportation networks [12]. Extensive effort was put forth for post-earthquake damage assessment and recovery, which illustrated the need for decision-making processes and early planning in Nepal [27]. Hence, it provided a suitable area for testing our new methodology.

### 3.1. Study area and data collection/processing

Individual researchers, governmental organizations, and universities volunteered to collect data for mapping landslides after the Gorkha disaster, either on-site or from satellite images [15,22]. For our research purposes, we compiled all of the available open-source landslide data from Durham University/British Geological Survey [15], the International Center for Integrated Mountain Development (ICIMOD), NGA, and the United Nations Institute for Training and Research (UNITAR-UNISAT) [41]. These data were presented under various types of formatting (e.g., points and/or lines). During a site visit in 2016, we also obtained data concerning the rural road network from the Department of Road Authority (DoR) in Nepal.

The road network of Sindhupalchok District comprises 457 nodes and 557 edges and was modeled as an undirected and weighted graph, which is mainly the case in geohazard-related emergencies. To identify road segments that were closed due to earthquake-triggered landslides in the study area, we overlaid the Sindhupalchok road layer with each of the landslide layers acquired from different resources and considered the intersected road segments to be affected by the disaster. It is found that a total of 66 road segments was closed due to the landslides. The road disruptions and landslide data are given in Fig. 4.

The clearing time of a blocked road segment depended on the magnitude of landslides (i.e., debris size due to landslide) blocking the road segment as well as the operational capacity of the road authorities to restore damaged segments. To determine the size of the blockage, landslides were classified as small, medium and large using the compiled data from the above-mentioned sources and the satellite images. Then, a survey conducted to determine a range of restoration time for

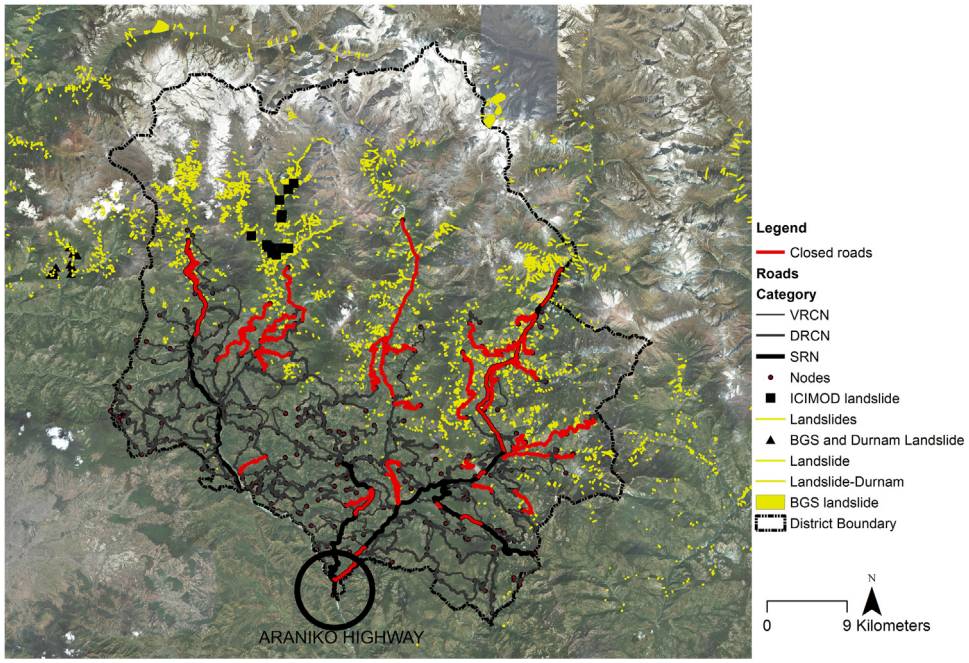


**Fig. 4.** Sindhupalchok road network and landslide data set. SRN: Strategic Road Network, VRCN: Village Road Core Network, and DRCN: District Road Core Network.

**Table 1**
Minimum and maximum time required to open disrupted road segments in Sindhupalchok District.

| Impact class | Impact measure | Repair time in hours | | | | |
|---|---|---|---|---|---|---|
| | | Lower bound | Upper bound | Mean | Standard deviation | Coefficient of variation |
| Very small | 0–2.5 | 1 | 3 | 2 | 0.4 | 0.2 |
| Small | 2.5–5 | 3 | 7 | 5 | 1 | 0.2 |
| Medium | 5–10 | 7 | 10 | 8.5 | 1.7 | 0.2 |
| High | 10–20 | 10 | 24 | 17 | 3.4 | 0.2 |
| Very high | 20–30 | 24 | 72 | 48 | 9.6 | 0.2 |

small, medium and large landslides. Surveys were conducted separately for both road authorities and public who were experiencing frequent road closure during their business and/or daily lives. Both surveys included questions for determining cleaning and opening time of blocked road segments due to the small, medium and large landslides. The separate surveys yielded consistent results about the road restoration time according to the landslide sizes, which provided a high level of confidence in using those collected data. Therefore, the results were used for assigning road-clearing times to road segments, which are blocked due to small, medium or large landslides. As a result, considering both surveys and the magnitude of hazards, the following assumptions were made when assigning the amount of time it would take to repair the disrupted road segments. Table 1 shows the average amount of time it takes to repair the disrupted road segments for a given landslide size.

In Table 1, the impact measure represents the size of debris due to a landslide that blocks the road segment, which determined road opening time. Here, the aerial extent and predicted volumes map of landslides after the earthquake were considered. Then, these areas were overlaid by the road network. The amount of debris and the length of the road segment were considered for classifying the impact measure. In this study, minimum, maximum, and mean recovery times were determined based on the results of field surveys. The coefficient of variation was assumed to be 0.2, which was obtained by the road-opening times declared in the surveys. This was used to calculate the standard deviation for the Monte Carlo simulations and was then applied as a parameter for the truncated normal PDF to characterize uncertainty in recovery times for Strategy 1.

### 3.2. Performance evaluation for strategies

All strategies were tested in terms of rebuilding connectivity over time by evaluating the GCC and normalizing it after restoring each closed segment (Eq. (1)). Interviews with authorities in Sindhupalchok District revealed that rescue, supply, and reconstruction personnel sent by the DoR came from south of the rural road network, marked as Araniko Highway in Fig. 4. This highway connects the district to the Kathmandu Metropolitan area. Therefore, all of the resilience enhancement strategies were designed based on proximity to that highway. In this study area, the entrance node, Araniko Highway, was considered the main “resource center” for restoration operations. Data from field studies indicated limitations in equipment availability and related human resources. Hence, it was assumed that only one recovery team could work on clearing the debris.

#### 3.2.1. Evaluation of Strategy 1

This strategy investigated recovery performance when disrupted roads were in close proximity to the main resource, Araniko Highway. Different PDFs were initially tested with Strategy 1 in order to determine which PDF would be used for all strategies. The results for drawing samples (i.e., 10,000 times) using three different distributions for restorations times are given in Fig. 5. The motivation for this test was to use a single distribution that represented a wider range of uncertainty for analysis of all strategies and to reduce overall computation time.

In Fig. 5, very similar results were acquired for the triangular and truncated normal PDFs (see also the histograms in Fig. 6). The uniform distribution provided the largest envelope and, therefore, a higher level of uncertainty with a wider range. Hence, Monte Carlo simulations for all strategies were evaluated by drawing random samples for recovery times with uniform distribution.

#### 3.2.2. Evaluation of Strategy 2

The Sindhupalchok rural road network entails three road

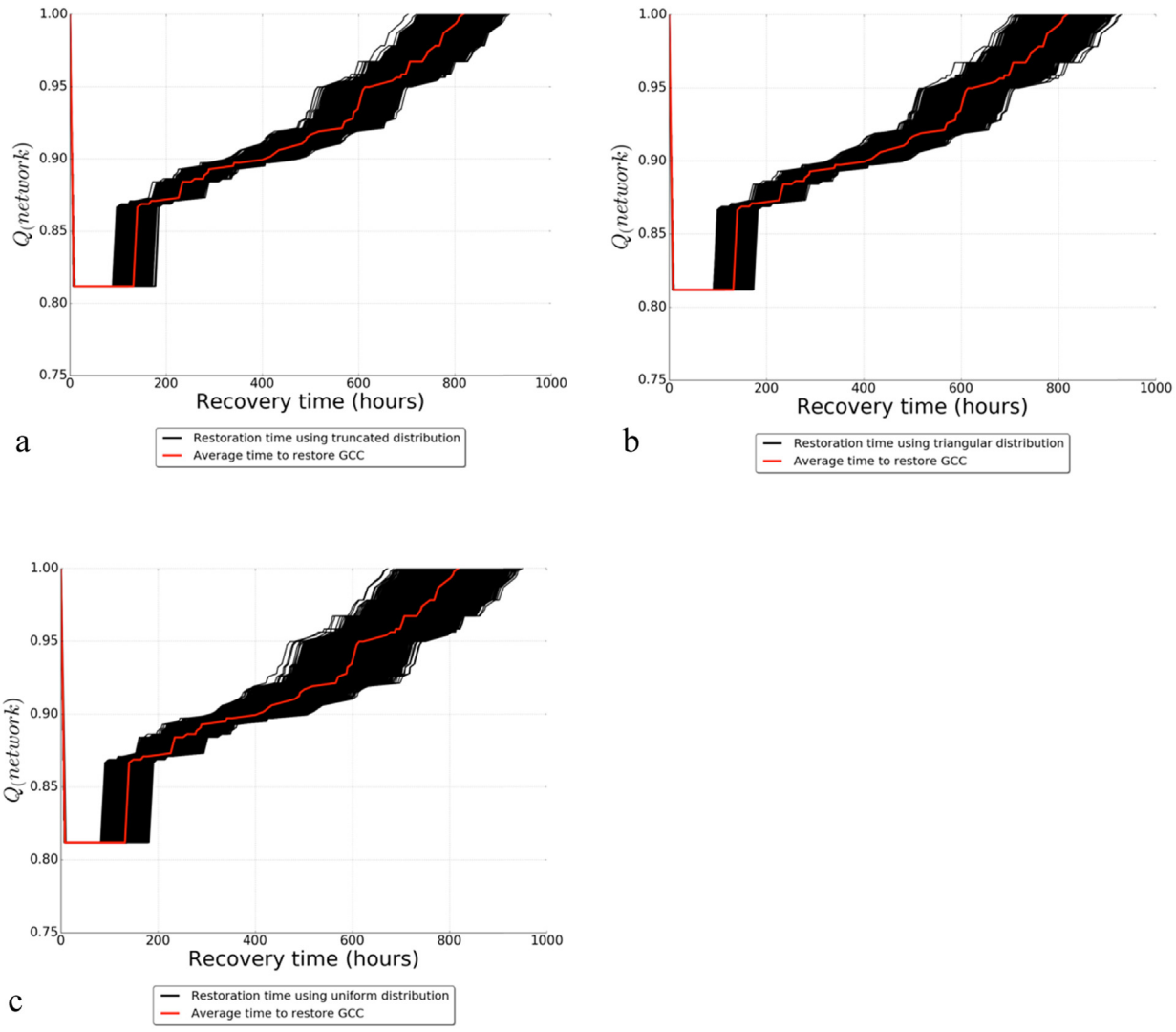


**Fig. 5.** Testing different distributions on recovery in Strategy 1: a) truncated normal distribution, b) triangular distribution, and c) uniform distribution.

hierarchies: SRN, VRCN, and DRCN (c.f., Fig. 4). The SRNs are the main road segments that connect major functions, main population centers, and even neighboring countries. In contrast, the DRCN is defined as the minimum network of rural roads that provides access to the Village Development Committees and/or district headquarters (e.g., administrative buildings, nearest economic centers). The VRCN is designed to provide access to settlements in the Village Development Committees [36].

Ideally, connecting major population centers would assist in increasing not only operational resilience but also community-level resilience after natural disasters. In this strategy, first, the closed SRN road segments were added back into the network. The sequence of adding these SRN edges was determined based on the proximity to the resource: Araniko Highway. The same procedure was applied to the closed DRCN and VRCN segments.

### 3.2.3. Evaluation of Strategy 3

This strategy featured a road recovery sequence based on proximity to Araniko Highway as well as the amount of time it would take to restore each segment, as indicated in Table 1. Rather than working on segments that needed more time, priority was given to segments that required less time to rebuild and that was closer to the resource center. Total recovery times were determined by adding each disrupted road segment back into the network and then, taking the cumulative sums of the corresponding time (i.e., in hours), which was repeated for 10,000 times. In, Strategy 1, the road recovery based on proximity to the main resource Araniko Highway performs the worst in terms of rapid recovery of connectivity. The connectivity performance of Strategy 3 called (time/proximity) was better than the other two strategies during the early days of activity (see blue line in Fig. 7). Although Strategy 2 performance exceeded Strategy 3 the following 10 days, (i.e., orange line in Fig. 7), Strategy 3 still performed better than Strategy 2 since the GCC performance was close to 1.

### 3.2.4. Evaluation of Strategy 4

Strategy 4 was primarily focused on the recovery performance of overall connectivity when accounting for the uncertainty in sequencing road segments. Here, unlike with Strategy 3, we omitted the proximity prerequisite and considered only the time variable (i.e., the output of Monte Carlo simulations). This approach would be helpful for decision-makers in terms of understanding the changes in recovery behavior under uncertainty. In the model, the road segments are unblocked based on the time it takes to recover them in ascending order. The results are given in Fig. 8, which indicates that the variability in connectivity performance varied more widely, as the sequences for opening road segments change based on time.

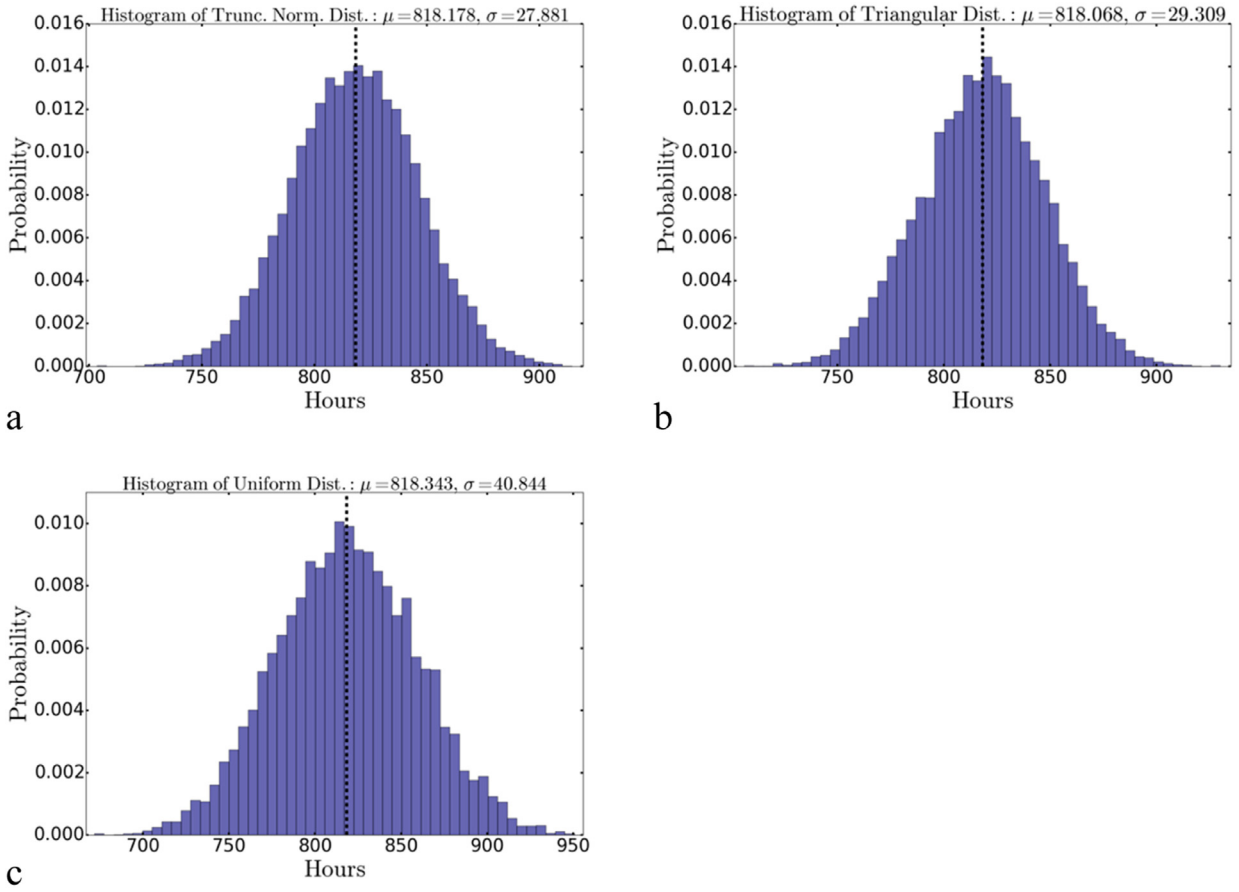


**Fig. 6.** Histograms for testing different distributions on Strategy 1, with bin size of 50. a) truncated normal distribution, b) triangular distribution, and c) uniform distribution.

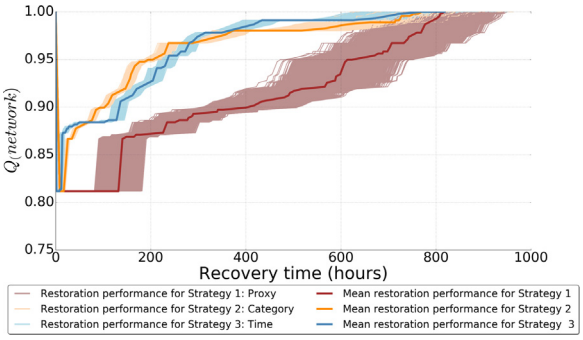


**Fig. 7.** Results from 10,000 simulations for Strategies 1, 2, and 3. Sequences for recovering road segments were selected according to criteria for individual strategies; times were randomly drawn based on uniform distribution.

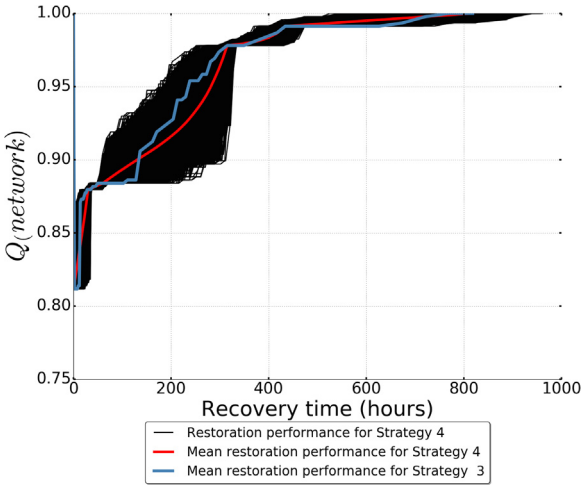


**Fig. 8.** Simulation results for Strategy 4: Time to recovery was determined by uniform distribution, and sequences for opening segments were updated accordingly.

## 4. Results and discussions

Our case study demonstrated that the most efficient strategy, in terms of rapidly restoring connectivity for the entire network, relied upon sequencing road segments based on the time variable. Histograms for the final recovery times for all strategies are given in Fig. 9.

The first proposed comparison criterion was *final mean recovery time*. Fig. 9 illustrates that the final mean recovery times of all strategies were approximately 818 h. Variability in results was insignificant among strategies. In addition, the probability of restoring all road segments in less than 800 h for Strategies 1, 2, 3, and 4 was 0.327, 0.333, 0.329, and 0.328, respectively. However, Figs. 7 and 8 clearly revealed differences in performance between strategies during the recovery process.

Our second comparison criterion was *efficiency in the recovery process*. CDFs were created to compare the mean recovery times necessary to unblock 25%, 50%, and 75% of all road segments (Figs. 10–12). In addition, Table 2 shows the probabilities of completing the recovery in less than 100, 300 and 500 h at 25%, 50%, and 75%. Table 2 also presents the probabilities of completing this recovery in less than 100, 300, and 500 h at completion levels of 25%, 50%, and 75%. Strategies 3 and 4 were the most favorable because they showed the highest probability of opening the road segments faster than the

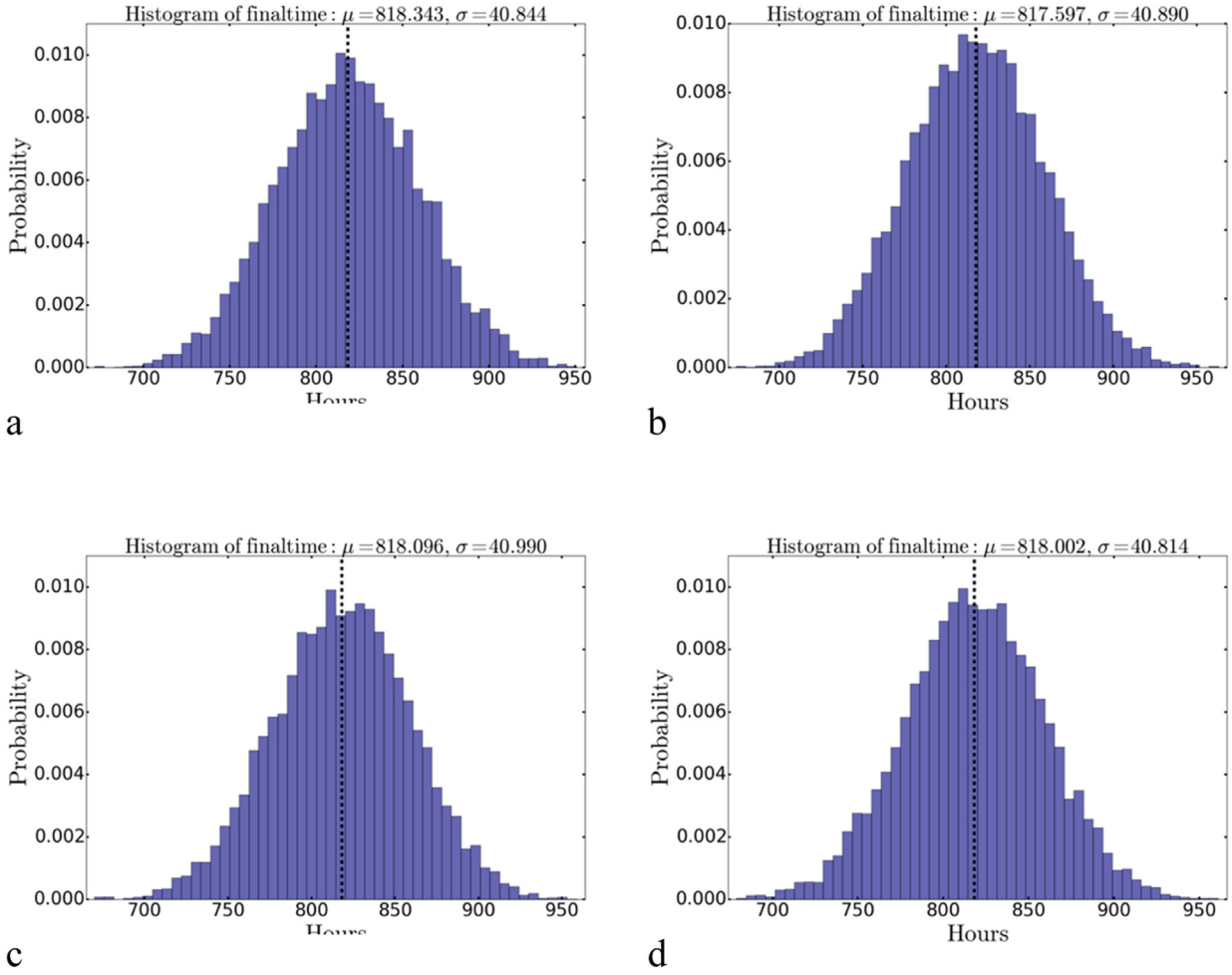


**Fig. 9.** Histograms representing final mean recovery times (100% of closed roads recovered) a) Strategy 1, b) Strategy 2, c) Strategy 3, and d) Strategy 4.

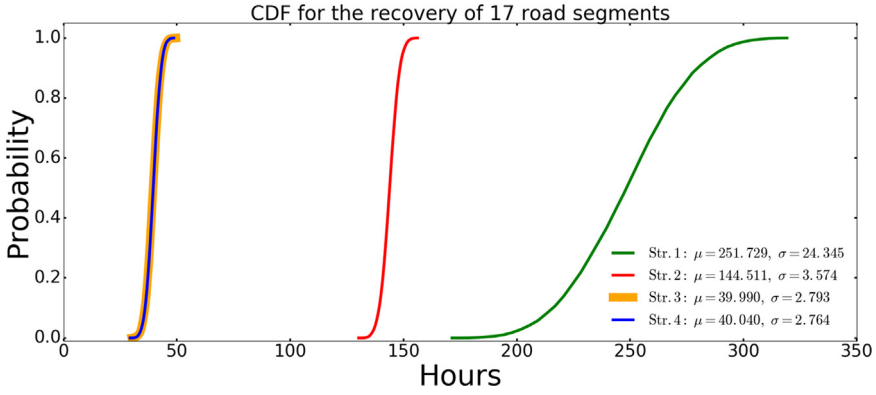


**Fig. 10.** CDFs representing recovery of 17 segments (25% of all closed roads).

other strategies. However, those two strategies did not differ significantly in their performances.

Finally, we compared the results with respect to *magnitude of uncertainty*, which was quantified according to minimum and maximum times at 25%, 50%, 75%, and 100% recovery (Table 3). At the stage of complete recovery, this magnitude was not significantly altered because changes in minimum and maximum recovery times and their 95% confidence intervals (CIs) were insignificant. The minimum and maximum range was smaller for Strategy 1 than for Strategies 3 and 4 at 100% level. However, at the 75%, 50%, and 25% levels, this condition changed significantly, and differences in performance for Strategies 3 and 4, when compared with the other two, were very clear.

In evaluating these four strategies, we were able to improve our understanding about road recovery behavior and performance as it relates to enhancing the operational resilience of a rural road network in the Sindhupalchok District of central Nepal. These comparisons were made based on final mean recovery times, efficiency during the recovery process, and the magnitude of uncertainty. Here, mean recovery times did not vary significantly among strategies (see p-values at 100% recovery in Table 2).

Nevertheless, we found significant differences in efficiency during the recovery process, as well as in the magnitude of uncertainty at the

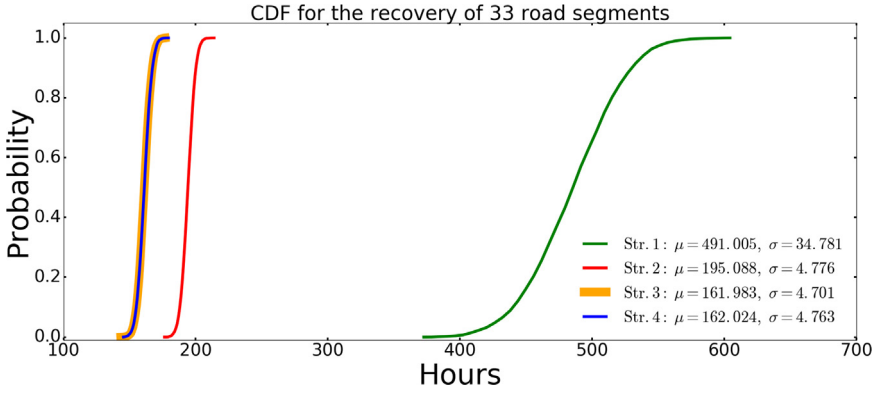


**Fig. 11.** CDFs representing recovery of 33 segments (50% of all closed roads).

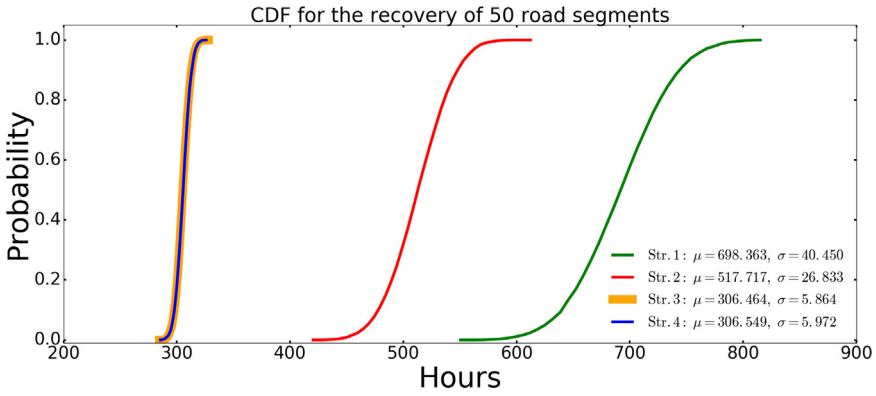


**Fig. 12.** CDFs representing recovery of 50 segments (75% of all closed roads).

**Table 2**
P-values for recovery processes.

| P-values | *Strategy 1* | *Strategy 2* | *Strategy 3* | *Strategy 4* |
|---|---|---|---|---|
| at 25%, < 100 h | 0 | 0 | 1 | 1 |
| at 50%, < 300 h | 0 | 1 | 1 | 1 |
| at 75%, < 500 h | 0 | 0.255 | 1 | 1 |
| at 100%, < 800 h | 0.327 | 0.333 | 0.329 | 0.330 |

**Table 3**
Statistical results for all strategies (times given in hours).

| **All road segments recovered (100%)** | *Strategy 1* | *Strategy 2* | *Strategy 3* | *Strategy 4* |
|---|---|---|---|---|
| Min recovery time | 672 | 674 | 670 | 679 |
| Max recovery time | 951 | 963 | 959 | 961 |
| Mean time | 818.34 | 817.60 | 818.10 | 818.00 |
| Std. deviation | 40.84 | 40.89 | 40.99 | 40.81 |
| 95% CI | [738.29, 898.40] | [737.46, 897.74] | [737.76,898.43] | [738.01, 898.00] |
| **75% of road segments recovered** | | | | |
| Min recovery time | 550 | 420 | 285 | 285 |
| Max recovery time | 822 | 617 | 329 | 327 |
| Mean time | 696.36 | 517.72 | 306.46 | 306.55 |
| Std. deviation | 40.45 | 26.83 | 5.86 | 5.97 |
| 95% CI | [619.08, 777.64] | [465.13, 570.31] | [294.97, 317.96] | [294.84, 318.25] |
| **50% of road segments recovered** | | | | |
| Min recovery time | 619 | 176 | 143 | 145 |
| Max recovery time | 373 | 215 | 178 | 180 |
| Mean time | 491.00 | 195.09 | 161.98 | 162.02 |
| Std. deviation | 34.78 | 4.78 | 4.70 | 4.76 |
| 95% CI | [422.84, 559.17] | [185.73, 204.45] | [152.77, 171.20] | [152.69, 171.36] |
| **25% of road segments recovered** | | | | |
| Min recovery time | 171 | 130 | 30 | 29 |
| Max recovery time | 323 | 157 | 50 | 49 |
| Mean time | 251.73 | 144.51 | 39.99 | 40.04 |
| Std. deviation | 24.35 | 3.57 | 2.79 | 2.76 |
| 95% CI | [204.01, 299.44] | [137.51, 151.52] | [34.51, 45.46] | [34.62, 45.46] |

point where 25%, 50%, or 75% of the blocked roads had been cleared (Tables 2 and 3). This indicated that strategy performances fluctuated during the recovery process, rather than having changes in overall recovery times. This is the case when all road segments are cleared. In our case study, road recovery strategies are evaluated to investigate the effects of different strategies on the recovery behavior, which supplies useful insight in enhancing operational resilience.

## 5. Conclusions

Evaluating the resilience of critical infrastructure systems requires measuring and understanding the complexity of systems operations and decision alternatives. This enables decision-makers to determine an acceptable level of operational capacity for a given infrastructure even if full capacity cannot be reached after a geohazard. Therefore, analysis and evaluation of decision alternatives for an agile recovery should be taken into account when designing operational resilience strategies, which includes involvement and interaction of various stakeholders.

Under ideal conditions, infrastructures such as transportation networks should be operational after major and multiple geohazards affect large areas of land (e.g., earthquakes, landslides triggered by earthquakes, or extreme weather events that lead to floods and landslides). The goal is to provide accessibility for relief efforts, thereby enhancing the resilience of a community. Cox [13] has highlighted the need to recognize interactions among community members when making

decisions about risk management.

The primary objective of our research was to develop a framework to evaluate road recovery strategies that could elucidate the unique recovery behavior of each strategy under uncertainty while also enhancing operational resilience and reducing associated complexities. Using a real-world scenario, we were successful in our implementation of this framework. This can now serve as a credible tool for decision-makers in assessing the implications of individual strategies on recovery functions. Our approach is sufficiently flexible so that those decision-makers can assign weights to different priorities (e.g., final mean recovery time, efficiency during the recovery process, or the magnitude of uncertainty) when selecting the most beneficial strategy. We found that the final mean recovery times did not differ significantly among strategies when 100% of the blocked segments were recovered. This would be a crucial factor if decision-makers and stakeholders preferred to recover only a part of the disrupted road network. In contrast, selecting criteria for efficiency during the recovery process and the magnitude of uncertainty clearly illustrated that resilience performance could differ among strategies.

We suggest that the sequencing of road segments based on the time needed for restoration would be the best strategy if the decision-makers' goal were efficiency during the recovery process. However, implementation of this strategy requires identifying the landslide magnitude and operation times, which could be effectively completed via (multi) hazard-susceptibility maps, even prior to those disruptions occurring.

Even though only four resilience enhancement strategies were analyzed in this study, that number could be increased based on the decision-makers' preferences. Regardless of the scale chosen, this methodology enables one to combine decision-making with analytical approaches. Chang et al. [11] have stated that infrastructure resilience is usually assessed as a systems-engineering problem that is solved through optimization. There, more focus is placed on technical aspects and specific threads for modeling physical losses. By comparison, our proposed framework evaluates several alternatives and associated uncertainties using topology-based and Monte Carlo simulations while also providing flexibility for decision-makers and organizations to investigate system-recovery strategies. It also allows them to observe the behavior of a strategy throughout the recovery process. Since rapid restoration of an infrastructure improves access for relief and rescue operations, such insight is crucial not only for boosting structural and operational resilience and recovery time over the entire network but also for the community that it serves.

In this study, recovery times were assigned to road segments using uniform, random sampling with Monte Carlo simulations. Minimum and maximum times to segment recovery were determined from field surveys and landslide intensity maps. However, in real-world situations, authorities and/or responders cannot necessarily show full performance to recover all road segments within a minimum amount of time. Therefore, Monte Carlo simulations are applied with a random draw of road recovery times that uses a uniform PDF. Those results then represent the uncertainties in each strategy and provide a more realistic solution for emergency management planning.

One limitation of this study could be the cost of allocating resources, a factor we did not consider in our current evaluation. This facet could be formulated as an optimization problem in future work. An important strategy for enhancing community resilience involves considering the population that would be affected by road blockages. Thus, planners could incorporate knowledge about the size of the population at each node when identifying which segments to open first. This strategy would require a detailed population dataset on a nodal scale. Because we lacked such information about the Sindhupalchok rural transportation network, we could not include that strategy in our investigation. However, assessment of that particular strategy would be more meaningful when analyzing the consequences of decisions that authorities would like to implement rather than always looking for the most efficient recovery strategy. Our proposed approach could also be modified to analyze such scenarios or decision-making problems. Although a comparison of debris-clearing approaches was not part of the scope of our study, it should be considered in future examinations.

Overall, our proposed methodology provides a new tool by which decision-makers and authorities can assess different recovery strategies and then enhance the resilience of their transportation networks. Not only does it simplify the process and improve the capacity to incorporate decision-makers' preferences, but it can also assist in planning and improving the resilience of transportation networks while materializing the theoretical resilience functions for a given network structure.

## Acknowledgement

This work was funded by a grant to N.Y.A. and H.R.H. from the National Research Foundation of Singapore (NRF) under its Campus for Research Excellence and Technological Enterprise (CREATE) programme (FI 370074011) for the Future Resilient Systems project at the Singapore-ETH Centre (SEC); and by an Alexander von Humboldt Foundation Georg Forster Experienced Researcher Fellowship Grant to H.S.D., hosted by F.W.

## References

[1] R. Albert, H. Jeong, A.-L. Barabasi, Error and attack tolerance of complex networks, Nature 406 (2000) 378–382.
[2] N.Y. Aydin, H.S. Duzgun, F. Wenzel, H.R. Heinimann, Integration of stress testing with graph theory to assess the resilience of urban road networks under seismic hazards, Nat. Hazards 91 (1) (2018) 37–68.
[3] B.M. Ayyub, Systems resilience for multihazard environments: definition, metrics, and valuation for decision making, Risk Anal. 34 (2) (2014) 340–355.
[4] H. Baroud, J.E. Ramirez-Marquez, K. Barker, C.M. Rocco, Stochastic measures of network resilience: applications to waterway commodity flows, Risk Anal. 34 (7) (2014) 1317–1335.
[5] D.N. Bristow, A.H. Hay, Graph model for probabilistic resilience and recovery planning of multi-infrastructure systems, J. Infrastruct. Syst. 23 (2017) 3.
[6] M. Bruneau, S.E. Chang, R.T. Eguchi, G.C. Lee, T.D. O'Rourke, A.M. Reinhorn, M. Shinozuka, K. Tierney, W.A. Wallace, D. von Winterfeldt, A framework to quantitatively assess and enhance the seismic resilience of communities, Earthq. Spectra 19 (4) (2003) 733–752.
[7] D.S. Callaway, M.E.J. Newman, S.H. Strogatz, D.J. Watts, Network robustness and fragility: percolation on random graphs, 2000. ⟨https://arxiv.org/abs/cond-mat/0007300v2⟩.
[8] M. Çelik, Ö. Ergun, P. Keskinocak, The post-disaster debris clearance problem under incomplete information, Oper. Res. 63 (1) (2015) 65–85.
[9] E.K. Çetinkaya, M.J.F. Alenazi, A.M. Peck, J.P. Rohrer, J.P.G. Sterbenz, Multilevel resilience analysis of transportation and communication networks, Telecommun. Syst. 60 (4) (2015) 515–537.
[10] S.E. Chang, Transportation planning for disasters: an accessibility approach, Environ. Plan. A 35 (6) (2003) 1051–1072.
[11] S.E. Chang, T. McDaniels, J. Fox, R. Dhariwal, H. Longstaff, Toward disaster-resilient cities: characterizing resilience of infrastructure systems with expert judgments, Risk Anal. 34 (3) (2014) 416–434.
[12] B.D. Collins, R.W. Jibson, Assessment of existing and potential landslide hazards resulting from the April 25, 2015 Gorkha, Nepal earthquake sequence, U.S. Dep. Inter. U.S. Geol. Surv. (2015).
[13] L.A. Cox Jr., Community resilience and decision theory challenges for catastrophic events, Risk Anal. 32 (11) (2012) 1919–1934.
[14] M. D'Lima, F. Medda, A new measure of resilience: an application to the London underground, Transp. Res. Part A: Policy Pract. 81 (2015) 35–46.
[15] Durham University, and British Geological Survey, Nepal earthquake landslide locations. D. University, and B. G. Survey, eds, 2016.
[16] W. Ellens, R.E. Kooij, Graph measures and network robustness, 2013. ⟨http://arxiv.org/abs/1311.5064v1⟩.
[17] K. Ertugay, S. Argyroudis, H.Ş. Düzgün, Accessibility modeling in earthquake case considering road closure probabilities: a case study of health and shelter service accessibility in Thessaloniki, Greece, Int. J. Disaster Risk Reduct. 17 (2016) 49–66.
[18] K. Ertugay, S. Duzgun, GIS-based stochastic modeling of physical accessibility using GPS-based floating car data and Monte Carlo simulation, Int. J. Geogr. Inf. Sci. 25 (9) (2011) 1491–1506.
[19] A.A. Ganin, E. Massaro, A. Gutfraind, N. Steen, J.M. Keisler, A. Kott, R. Mangoubi, I. Linkov, Operational resilience: concepts, design and analysis, Sci. Rep. 6 (2016) 19540.
[20] M.T. Gastner, M.E.J. Newman, The spatial structure of networks, Eur. Phys. J. 49 (2006) 247–252.
[21] I. Gidaris, J.E. Padgett, A.R. Barbosa, S. Chen, D. Cox, B. Webb, A. Cerato, Multiple-Hazard fragility and restoration models of highway bridges for regional risk and

resilience assessment in the United States: state-of-the-art review, J. Struct. Eng. 143 (3) (2017) 04016188.
[22] Gnyawali K.R., Adhikari B.R. (2017) Spatial Relations of Earthquake Induced Landslides Triggered by 2015 Gorkha Earthquake Mw = 7.8. In: Mikoš M., Casagli N., Yin Y., Sassa K. (eds) Advancing Culture of Living with Landslides. WLF 2017. Springer, Cham.
[23] T.H. Grubesic, T.C. Matisziw, A.T. Murray, D. Snediker, Comparative approaches for assessing network vulnerability, Int. Reg. Sci. Rev. 31 (1) (2008) 88–112.
[24] igraph. The network analysis package, 2017. 〈http://igraph.org/redirect.html〉 (16 March 2017).
[25] S. Iqbal, M. Usama Sardar, F.K. Lodhi, O. Hasan, Statistical model checking of relief supply location and distribution in natural disaster management, Int. J. Disaster Risk Reduct. (2018).
[26] H.W. Kua, On life cycle sustainability unified analysis, J. Ind. Ecol. 21 (6) (2017) 1488–1506.
[27] D. Lallemant, R. Soden, S. Rubinyi, S. Loos, K. Barns, G. Bhattacherjee, Post-disaster damage assessments as catalysts for recovery: a look at assessments conducted in the wake of the 2015 earthquake in Nepal, Earthq. Spectra (2017).
[28] J.C. Lam, B.T. Adey, Functional loss assessment and restoration analysis to quantify indirect consequences of hazards, Asce-Asme J. Risk Uncertain. Eng. Syst. Part A-Civil. Eng. 2 (2016) 4.
[29] V. Latora, M. Marchiori, Efficient behavior of small-world networks, Phys. Rev. Lett. 87 (19) (2001) 198701.
[30] P. Maya Duque, K. Sörensen, A GRASP metaheuristic to improve accessibility after a disaster, OR Spectr. 33 (3) (2011) 525–542.
[31] National Academy of Sciences, Disaster Resilience A national Imperative, The National Academies Press, Washington, D.C, 2012.
[32] J.R. Nelson, T.H. Grubesic, A repeated sampling method for oil spill impact uncertainty and interpolation, Int. J. Disaster Risk Reduct. 22 (2017) 420–430.
[33] M.E.J. Newman, The structure and function of complex networks, SIAM Rev. 45 (2) (2003) 167–256.
[34] M.E.J. Newman, Networks: An Introduction, Oxford University Press, Oxford, UK, 2010.
[35] F. Prager, Z. Chen, A. Rose, Estimating and comparing economic consequences of multiple threats: a reduced-form computable general equilibrium approach, Int. J. Disaster Risk Reduct. 31 (2018) 45–57.
[36] Rural Access Programme, DTMP Guielines for the Preparation of the Districti Transport Master Plan (DTMP), 2012.
[37] L.A. Schintler, R. Kulkarni, S. Gorman, R. Stough, Using raster-based GIS and graph theory to analyze complex networks, Netw. Spat. Econ. 7 (4) (2007) 301–313.
[38] Y. Shangyao, J.C. Chu, S. Yu-Lin, Optimal scheduling for highway emergency repairs under large-scale supply-demand perturbations, IEEE Trans. Intell. Transp. Syst. 15 (6) (2014) 2378–x2393.
[39] D. Tuzun Aksu, L. Ozdamar, A mathematical model for post-disaster road restoration: enabling accessibility and evacuation, Transp. Res. Part E: Logist. Transp. Rev. 61 (2014) 56–67.
[40] United Nations, Sendai Framework for Disaster Risk Reduction 2015–2030. Sendai, Japan, 2015.
[41] UNOSAT and NGA. UNOSAT LIVE Map: Nepal Earthquake. U. U. N. i. f. T. a. Research, ed, 2015.
[42] O. Woolley-Meza, C. Thiemann, D. Grady, J.J. Lee, H. Seebens, B. Blasius, D. Brockmann, Complexity in human transportation networks: a comparative analysis of worldwide air transportation and global cargo-ship movements, Eur. Phys. J. B 84 (4) (2011) 589–600.
[43] S. Yan, C.K. Lin, S.Y. Chen, Optimal scheduling of logistical support for an emergency roadway repair work schedule, Eng. Optim. 44 (9) (2012) 1035–1055.
[44] S. Yang, F. Hu, R.G. Thompson, W. Wang, Y. Li, S. Li, W. Ni, Criticality ranking for components of a transportation network at risk from tropical cyclones, Int. J. Disaster Risk Reduct. 28 (2018) 43–55.
[45] Y. Yang, Y. Liu, M. Zhou, F. Li, C. Sun, Robustness assessment of urban rail transit based on complex network theory: a case study of the Beijing Subway, Saf. Sci. 79 (2015) 149–162.
[46] D.W. Zhao, L.H. Wang, Y.F. Zhi, J. Zhang, Z. Wang, The robustness of multiplex networks under layer node-based attack, Sci. Rep. 6 (2016) 24304.